



DØ Note 4380-CONF

Search for Squarks and Gluinos in the Jets + Missing E_T topology

The DØ Collaboration
URL: <http://www-d0.fnal.gov>

(Dated: April 1, 2004)

A search for squarks and gluinos has been performed in 85 pb^{-1} of data from $p\bar{p}$ collisions at a center-of-mass energy of 1.96 TeV, collected by the DØ detector at the Fermilab Tevatron. The topology analysed consists of acoplanar jets with large missing E_T . The data show good agreement with the standard model expectations. Improved mass limits for squarks and gluinos have been derived in the framework of minimal supergravity.

Preliminary Results for Winter 2004 Conferences

I. INTRODUCTION

Topologies involving jets and missing transverse energy have been widely investigated in the past to search for signals of new phenomena in $p\bar{p}$ collisions. In this note, a search for squarks and gluinos in the acoplanar jet topology is reported, using 85 pb^{-1} of data collected at a center-of-mass energy of 1.96 TeV with the upgraded DØ detector during Run II of the Fermilab Tevatron.

In models based on theories of supersymmetry, scalar quarks, or squarks, arise as partners of the ordinary quarks. Supersymmetric particles carry a value of -1 for R -parity, a multiplicative quantum number. In R -parity conserving theories, supersymmetric particles are therefore produced in pairs. Their decay leads to Standard Model (SM) particles and, possibly via cascades, to the lightest supersymmetric particle (LSP) which is stable. The widely preferred LSP candidate is the lightest neutralino χ_1^0 , which is weakly interacting and thus escapes detection. (The neutralinos are the supersymmetric partners of the neutral gauge and Higgs bosons.)

At hadron colliders, the most copiously produced supersymmetric particles should be, if sufficiently light, colored particles, namely squarks and gluinos (the supersymmetric partners of the gluons). If squarks are lighter than gluinos, they will tend to decay according to $\tilde{q} \rightarrow q\chi_1^0$, and their pair production will yield an acoplanar jet topology with missing E_T carried away by the two neutralino LSP's. On the other hand, if gluinos are lighter than squarks, their pair production and decay *via* $\tilde{g} \rightarrow q\bar{q}\chi_1^0$ will lead to topologies containing a large number of jets and missing E_T . In generic models, squarks of the four lightest flavors tend to be of similar masses. The same is true for the supersymmetric partners of both quark helicity states. Hence, the cross section of squark pair production corresponds effectively to the sum of the productions of eight squark species. The current squark mass limits are of the order of $290\text{ GeV}/c^2$ for gluino masses of $310\text{ GeV}/c^2$, with some dependence on model parameters [1, 2]. Here and in the following, all limits quoted are at the 95% confidence level.

In this note, squark and gluino production is investigated in a configuration where squarks are lighter than gluinos. More specifically, the framework of the analysis is minimal supergravity (mSUGRA) [3], with parameters ($m_0 \ll m_{1/2}$) where this mass hierarchy is encountered. All results reported are preliminary.

II. DATA SAMPLE

For the studies reported in this note, an integrated luminosity of $\sim 110\text{ pb}^{-1}$, collected from April to September 2003, has been analysed. The Jets + \cancel{E}_T trigger used was not available previously in Run II. At the first level, it selects events in which at least three trigger towers record a transverse energy in excess of 5 GeV. At the second and third trigger levels, requirements are placed on \cancel{H}_T , the transverse energy missing to the reconstructed jets ($\cancel{H}_T = |\sum_{jets} \vec{p}_T|$). The \cancel{H}_T thresholds are 20 and 30 GeV at Levels 2 and 3, respectively.

For the subsequent data selection, it was required that no major component of the detector show any sign of degraded performance. This leaves an available total integrated luminosity of 85 pb^{-1} . The offline analysis utilizes jets reconstructed with the Run II cone algorithm, with a radius of 0.5 in η - ϕ space, appropriately corrected for the jet energy scale. The so-called good jets are further selected by general quality criteria essentially based on the jet transverse and longitudinal profiles.

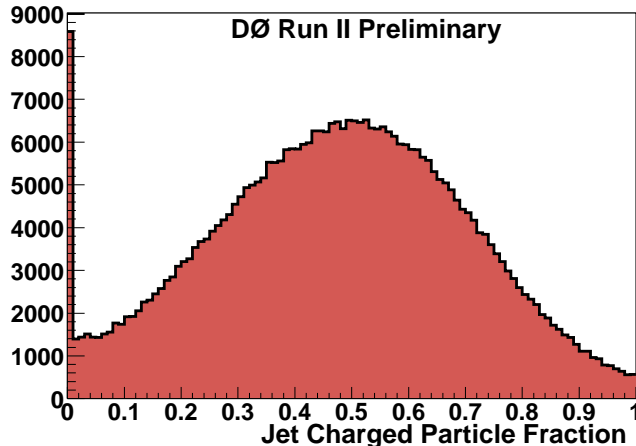
The sample of ~ 7 million events collected with the Jets + \cancel{E}_T trigger was reduced to a more manageable size by requiring the following criteria to be satisfied:

- $\cancel{H}_T > 40\text{ GeV}$;
- at least two jets;
- $p_{T1} > 40\text{ GeV}/c$;
- $|\eta_{\text{det1}}| < 1.5$;
- $\Delta\Phi < 165^\circ$,

where p_{T1} is the transverse momentum of the leading jet, η_{det1} is the leading jet pseudorapidity, assuming that the jet originates from the detector center, and $\Delta\Phi$ is the azimuthal angle between the two leading jets. Here and in the following, the qualifier “good” in front of “jet” is dropped; it will be restored only in case of ambiguities. Only good jets enter the calculation of kinematic quantities such as \cancel{H}_T or $\Delta\Phi$.

Events in which the presence of obvious calorimeter noise could be detected were rejected, as well as those containing at least one jet not rated as good and with a transverse energy larger than 15 GeV. The inefficiency of 3.4% associated with these criteria was measured on events selected at random beam crossings (zero-bias events), and also on events collected with an unbiased trigger and containing exactly two jets back-to-back in Φ within 15° .

FIG. 1: Distribution of the charged particle fraction CPF for central jets.



At this point, 328,156 events survive. This sample is still dominated by QCD events with jet transverse energy mismeasurements. Such mismeasurements can in particular be due to a wrong vertex choice, or to cosmic rays showering in the calorimeter. The improved tracking capabilities of the upgraded DØ detector can be used to largely reduce these backgrounds.

First the longitudinal position z of the vertex is restricted to ensure an efficient primary vertex reconstruction: $|z| < 60$ cm. This cut removes 3.9% of the events. Next a comparison of jet energies with their counterparts carried by charged particles is performed. The ratio CPF of the transverse energy carried by the charged particles associated with a jet to its transverse energy recorded in the calorimeter is expected to be close to zero either if a wrong primary vertex was selected, in which case it is unlikely that the charged tracks truly associated to the jet will emanate from the selected primary vertex, or if the jet is a fake one, in which case there should be no real charged tracks associated with it. The CPF distribution is shown in Fig. 1 for jets in events selected with an unbiased trigger. A jet is hereafter considered “confirmed” if its CPF is larger than 0.05.

The inefficiency of this jet confirmation procedure was determined using back-to-back dijet events with both jets required to be central ($|\eta_{\text{det}}| < 1$). From the fractions of events with 0, 1, or 2 jets confirmed, it is deduced that the chosen vertex is the correct one in 99% of the cases, and that track confirmation of a jet then occurs at a rate of 98% within $|\eta_{\text{det}}| < 1$. It has been checked that this efficiency does not depend on the jet p_T within the range of interest for the analysis reported in this note.

III. SIMULATED SAMPLES

Signal efficiencies and non-QCD standard model backgrounds have been evaluated using fully simulated and reconstructed Monte Carlo events, in which the jet energies received an additional smearing to take into account the different resolutions in data and Monte Carlo. The QCD background has not been simulated, and was estimated directly from the data.

A. Standard model background simulation

The processes listed in Table I are expected to be the largest contributors to standard model backgrounds in the acoplanar jet topology. They were generated with ALPGEN, interfaced with PYTHIA for the simulation of initial and final state radiation and of jet hadronization. The parton density functions (PDF’s) used were CTEQ6L and CTEQ5L, depending on the process. An average of 0.8 minimum bias events was superimposed.

The following requirements were imposed at the ALPGEN generator level:

- quark or gluon parton $p_T > 8 \text{ GeV}/c$;
- $\Delta R > 0.4$ for all angles between quarks and/or gluons.

TABLE I: Standard model processes, numbers of events generated and cross sections.

SM process	events generated	cross section (pb)
$Z \rightarrow \nu\bar{\nu} + \text{jet jet}$	43 683	144
$W \rightarrow \tau\nu + \text{jet}$	49 500	732
$W \rightarrow \tau\nu + \text{jet jet}$	32 224	255
$W \rightarrow \mu\nu + \text{jet jet}$	188 000	255
$W \rightarrow e\nu + \text{jet}$	95 750	732
$W \rightarrow e\nu + \text{jet jet}$	189 500	255
$Z \rightarrow \tau\tau + \text{jet}$	50 000	72
$Z \rightarrow \mu\mu + \text{jet jet}$	188 000	26

TABLE II: Chosen $m_{1/2}$ values, corresponding average-squark and gluino masses in GeV/c^2 , and total squark-and-gluino production cross sections.

$m_{1/2}$	$m_{\tilde{q}}$	$m_{\tilde{g}}$	cross section (pb)
100	228	260	9.5
105	238	270	7.1
110	250	284	5.0
115	259	296	3.8
120	269	306	2.8
125	280	319	2.1
130	290	332	1.5
135	299	340	1.2
140	310	353	0.9

In order to avoid double counting among the various samples, the numbers of jets reconstructed from the generated particles were required to be equal to the corresponding numbers of partons requested whenever a similar sample with higher requested jet multiplicity was available.

B. Signal simulation

The production of squarks and gluinos *via* the processes

$$q\bar{q} \text{ or } gg \rightarrow \tilde{q}\tilde{q}^* \text{ or } \tilde{g}\tilde{g}$$

$$qq \rightarrow \tilde{q}\tilde{q}$$

$$qg \rightarrow \tilde{q}\tilde{g}$$

was simulated using PYTHIA with the CTEQ5L PDF's. An average of 0.8 minimum bias events was overlaid.

The mSUGRA parameters were chosen at the boundary of the Run I exclusion domain for squarks lighter than gluinos: $m_0 = 25 \text{ GeV}/c^2$, $\tan\beta = 3$, $A_0 = 0$, $\mu < 0$, and $m_{1/2}$ in the range 100 to 140 GeV/c^2 , in 5 GeV/c^2 steps. In each case, a sample of 5 000 events was generated. The physical masses were calculated with the ISAJET version 7.58 package [5], and the cross sections by PYTHIA with K-factors for the various production processes given by PROSPINO [4] (Table II). All decay channels are implemented in the generator, including cascade decays such as $\tilde{q} \rightarrow \chi_1^\pm q \rightarrow qq\chi_1^0$ which reduce the efficiency of a search for acoplanar jets. Only squarks belonging to the first two generations were considered in this study.

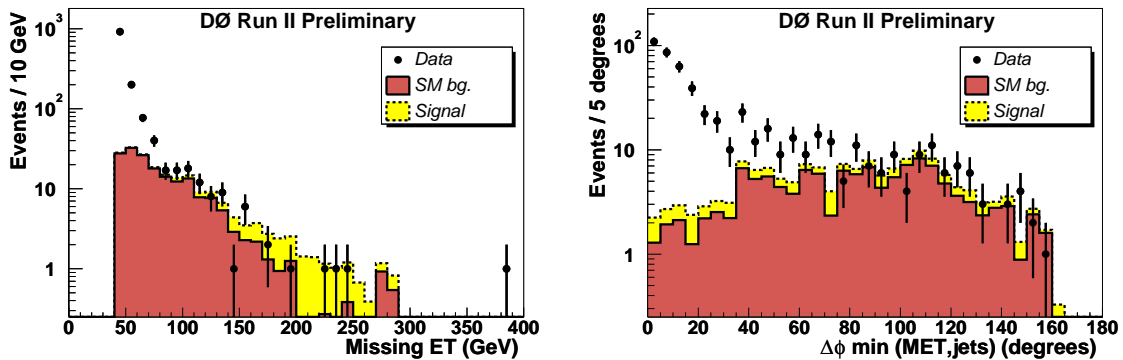
IV. EVENT SELECTION

The selection cuts which have been applied in this analysis are listed in Table III, together with the numbers of events surviving at each step and with the evolution of the efficiency for signal events close to the expected sensitivity limit.

The kinematic cuts **C1**, **C2** and **C3** reject a large fraction of the standard model backgrounds (including QCD), at the expense of a moderate signal inefficiency. The purpose of cuts **C4** and **C6** is to reject events likely to contain an isolated energetic electron. (EMF is the fraction of jet energy contained in the electromagnetic section

TABLE III: Numbers of data events selected and signal efficiencies for $m_{1/2} = 130 \text{ GeV}/c^2$ at the various stages of the analysis.

cut applied	events left	efficiency (%)
Initial cuts	328 156	70.3
C1 : leading jet $p_{T1} > 60 \text{ GeV}/c$	215 082	69.9
C2 : leading jet $ \eta_{\text{det}} < 0.8$	163 603	53.9
C3 : second leading jet $p_{T2} > 50 \text{ GeV}/c$	44 694	46.0
C4 : both leading jet EMF < 0.95	44 421	45.1
C5 : leading or second leading jet CPF > 0.05	38 692	42.3
C6 : no electromagnetic object with $p_T > 10 \text{ GeV}/c$	38 550	39.2
C7 : no isolated muon with $p_T > 10 \text{ GeV}/c$	37 780	33.7
C8 : missing $E_T > 60 \text{ GeV}$	1529	32.4
C9 : minimum $\Delta\Phi_{(E_T, \text{jet})} > 30^\circ$	411	25.8
C10 : maximum $\Delta\Phi_{(E_T, \text{jet})} < 165^\circ$	212	18.8
C11 : Optimized cuts ($\cancel{E}_T > 175 \text{ GeV}$ and $H_T > 275 \text{ GeV}$)	4	6.6

FIG. 2: Distribution of \cancel{E}_T after all cuts except **C11** and with **C8** relaxed (left) and of the minimum $\Delta\Phi_{(E_T, \text{jet})}$ after all cuts except **C9** and **C11** for data (points with error bars), for non-QCD standard model background (full histogram), and for signal Monte Carlo ($m_{1/2} = 130 \text{ GeV}/c^2$; dashed histogram on top of SM).

of the calorimeter.) Together with cut **C7**, they reject a large fraction of events originating from the $W/Z + \text{jet(s)}$ processes. The motivation for cut **C5** has been discussed previously.

The purpose of cuts **C8**, **C9** and **C10** is still to reject QCD background events in which the missing E_T is expected either to be moderate, or to be correlated with the direction of one of the jets in the event. The effect of cuts **C8** and **C9** is shown in Fig.2 for the data, the standard model background and a typical signal.

The final selection is based on two variables: \cancel{E}_T and H_T , where H_T is the sum of the transverse energies of all the jets in the event. The correlation between \cancel{E}_T and H_T is displayed in Fig.3 for data, standard model backgrounds and signal for $m_{1/2} = 130 \text{ GeV}/c^2$.

For various combinations of cut values on \cancel{E}_T and H_T , the expected cross section upper limit \mathcal{S} , scaled to the theoretical cross section for $m_{1/2} = 130 \text{ GeV}/c^2$, was determined, assuming that the number of events observed would be the one expected from background, and taking the systematic uncertainties discussed further down into account. The optimal set of cuts is the one which minimizes \mathcal{S} :

- $\cancel{E}_T > 175 \text{ GeV}$;
- $H_T > 275 \text{ GeV}$.

Four events were selected in the data.

V. BACKGROUNDS

For the optimized set of cuts, the various standard model background contributions are listed in Table IV. The main contributor is, as expected, $Z \rightarrow \nu\bar{\nu} + \text{jet jet}$.

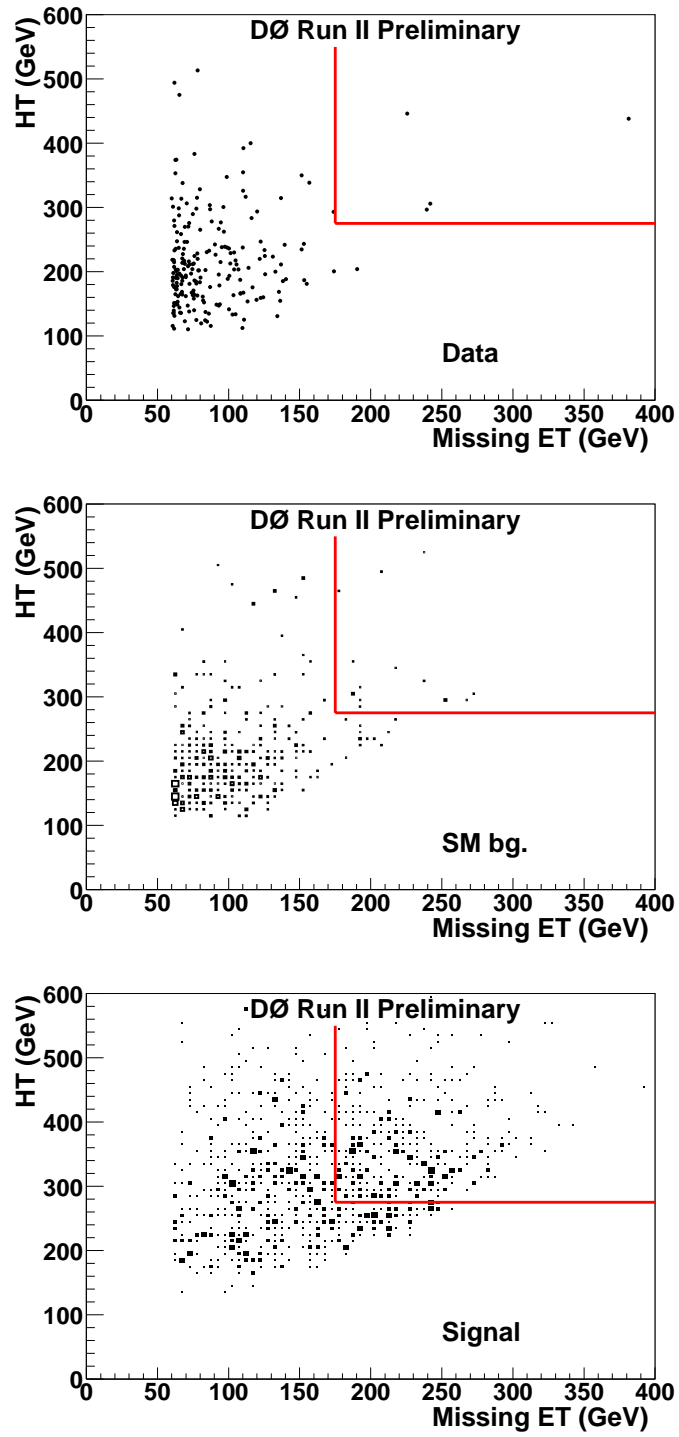


FIG. 3: Distribution of H_T vs. \cancel{E}_T after all cuts except **C11** for data (top), for non-QCD standard model background (middle), and for signal Monte Carlo ($m_{1/2} = 130 \text{ GeV}/c^2$) (bottom). The optimized \cancel{E}_T and H_T cuts are indicated.

TABLE IV: Standard model processes and numbers of events expected for the optimized set of cuts. The errors on the numbers of events expected are statistical only.

SM process	events expected
$Z \rightarrow \nu\bar{\nu} + \text{jet jet}$	1.35 ± 0.62
$W \rightarrow \tau\nu + \text{jet}$	0
$W \rightarrow \tau\nu + \text{jet jet}$	0.65 ± 0.66
$W \rightarrow \mu\nu + \text{jet jet}$	0.45 ± 0.23
$W \rightarrow e\nu + \text{jet}$	0
$W \rightarrow e\nu + \text{jet jet}$	0.22 ± 0.16
$Z \rightarrow \tau\tau + \text{jet}$	0
$Z \rightarrow \mu\mu + \text{jet jet}$	0
total	2.67 ± 0.95

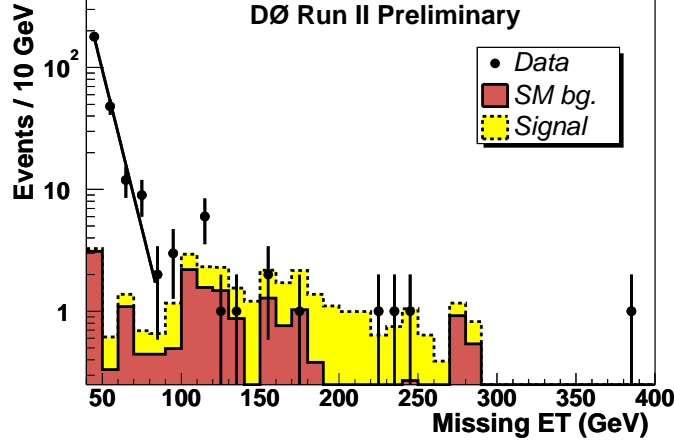


FIG. 4: Distribution of \cancel{E}_T after all cuts, except for the final cut on \cancel{E}_T , for data (points with error bars), for non-QCD standard model background (full histogram), and for signal Monte Carlo ($m_{1/2} = 130 \text{ GeV}/c^2$; dashed histogram on top of SM). The fitted QCD background is also drawn.

The QCD background was estimated, for the chosen H_T cut of 275 GeV, from an exponential fit to the lower bins of the missing E_T distribution (Fig. 4). For $\cancel{E}_T > 175 \text{ GeV}$, the QCD background is found to be totally negligible.

VI. RESULTS

A. Signal efficiency

The signal efficiencies were evaluated using fully simulated events. For the events fulfilling all the selection criteria, it was verified that the trigger inefficiencies are negligible. The evolution of the efficiency at the various stages of the analysis is given in Table III for $m_{1/2} = 130 \text{ GeV}/c^2$. The final efficiencies for various $m_{1/2}$ values are displayed in Table V.

B. Systematic uncertainties

The main experimental systematic errors are fully correlated between signal and SM backgrounds:

- a 6.5% uncertainty on the integrated luminosity;
- the uncertainties in the data and Monte Carlo jet energy scales. These were added in quadrature and yield a $^{+20}_{-15}\%$ relative uncertainty on the signal efficiency, and a $^{+77}_{-43}\%$ uncertainty on the SM background prediction.

TABLE V: Signal efficiency and number of events expected for various values of $m_{1/2}$. The errors are statistical only.

$m_{1/2}$ (GeV/ c^2)	efficiency (%)	events expected
100	2.13 ± 0.20	17.1 ± 1.6
105	2.63 ± 0.23	15.0 ± 1.4
110	3.34 ± 0.25	14.2 ± 1.1
115	3.56 ± 0.28	11.4 ± 0.9
120	4.27 ± 0.29	10.2 ± 0.7
125	5.49 ± 0.32	9.8 ± 0.6
130	6.55 ± 0.35	8.4 ± 0.5
135	5.90 ± 0.33	5.5 ± 0.3
140	7.10 ± 0.44	4.8 ± 0.3

TABLE VI: Kinematic properties of the event with the largest missing E_T . Energies are in GeV, momenta in GeV/ c , and angles in radians.

	p_T	η	ϕ
\cancel{E}_T	381		2.25
H_T	431		
Jet 1	289	-0.21	5.66
Jet 2	117	0.54	4.78
Jet 3	14	-1.55	4.27
Jet 4	11	-0.09	1.58

The systematic errors on the signal cross sections, of the order of 10%, were taken from Ref. [4]. Those affecting the SM background cross sections, of the order of 8%, have been estimated by varying in ALPGEN the set of PDF's used and the renormalization scale.

C. Limits

Given

- the observation of four events,
- the background expectation of 2.7 ± 0.95 events,
- the signal efficiencies given in Table V,
- the above discussed systematic uncertainties, and
- the integrated luminosity of $85.1 \pm 5.5 \text{ pb}^{-1}$,

cross section upper limits have been obtained for the sets of mSUGRA parameters considered, using the CL_s approach [6] with correlations between systematic errors properly taken into account. The result is displayed in Fig.5. For $m_0 = 25 \text{ GeV}/c^2$, all $m_{1/2}$ values smaller than $131 \text{ GeV}/c^2$ are excluded, which corresponds to a gluino mass of $333 \text{ GeV}/c^2$ for a squark mass of $292 \text{ GeV}/c^2$. The corresponding most probable gluino-mass limit expected in this analysis is $338 \text{ GeV}/c^2$. For the same squark-mass value, the most constraining limit on the gluino mass obtained with Run I data was $\sim 310 \text{ GeV}/c^2$ [2].

The kinematic properties of the event with the largest missing E_T are given in Table VI. Displays are presented in Fig. 6.

Acknowledgments

We thank the staffs at Fermilab and collaborating institutions, and acknowledge support from the Department of Energy and National Science Foundation (USA), Commissariat à L'Energie Atomique and CNRS/Institut National de Physique Nucléaire et de Physique des Particules (France), Ministry for Science and Technology and Ministry for

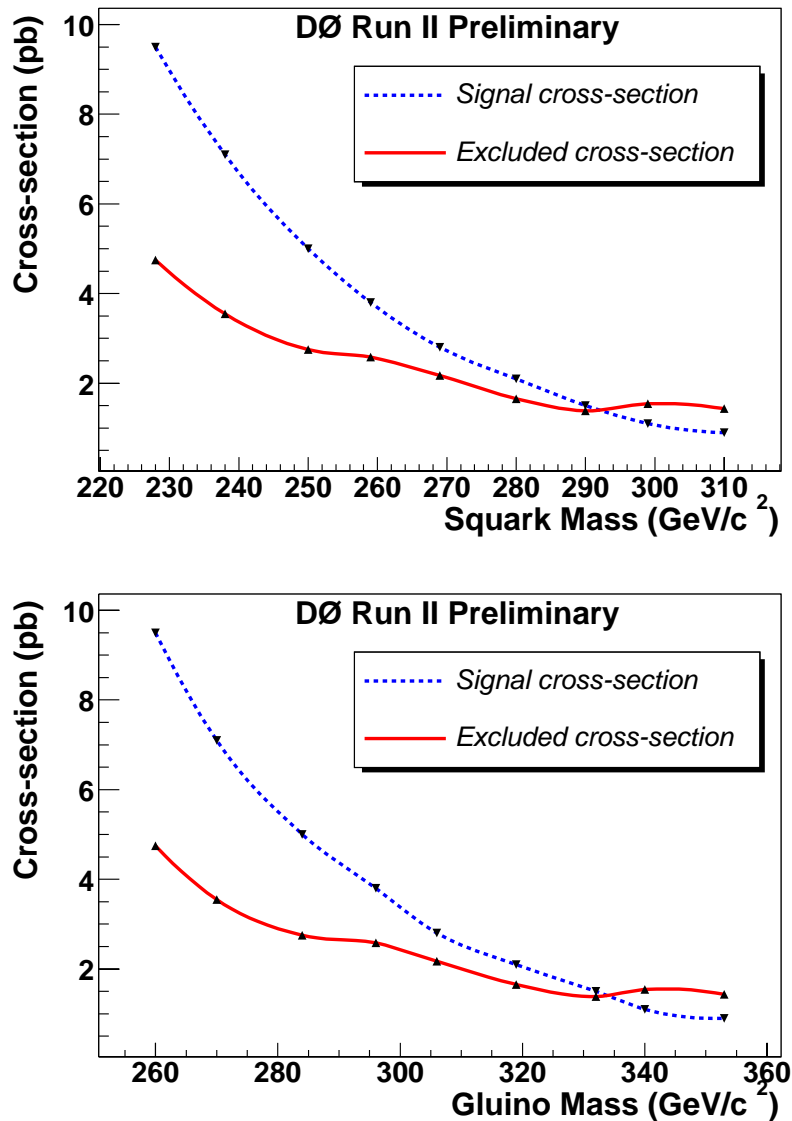


FIG. 5: Squark-and-gluino production cross section upper limit as a function of the average-squark (top) and gluino (bottom) masses (full curve, red), and theoretical expectation (dashed curve, blue) for $m_0 = 25 \text{ GeV}/c^2$, $A_0 = 0$, $\tan \beta = 3$ and $\mu < 0$.

Atomic Energy (Russia), CAPES, CNPq and FAPERJ (Brazil), Departments of Atomic Energy and Science and Education (India), Colciencias (Colombia), CONACyT (Mexico), Ministry of Education and KOSEF (Korea), CONICET and UBACyT (Argentina), The Foundation for Fundamental Research on Matter (The Netherlands), PPARC (United Kingdom), Ministry of Education (Czech Republic), Natural Sciences and Engineering Research Council and West-Grid Project (Canada), BMBF (Germany), A.P. Sloan Foundation, Civilian Research and Development Foundation, Research Corporation, Texas Advanced Research Program, and the Alexander von Humboldt Foundation.

-
- [1] DØ Collaboration, B. Abbott *et al.*, “Search for Squarks and Gluinos in Events Containing Jets and a Large Imbalance in Transverse Momentum”, Phys. Rev. Lett. **83** (1999) 4937.
 [2] CDF Collaboration, T. Affolter *et al.*, “Search for Gluinos and Scalar Quarks in $p\bar{p}$ Collisions at $\sqrt{s} = 1.8 \text{ TeV}$ using the

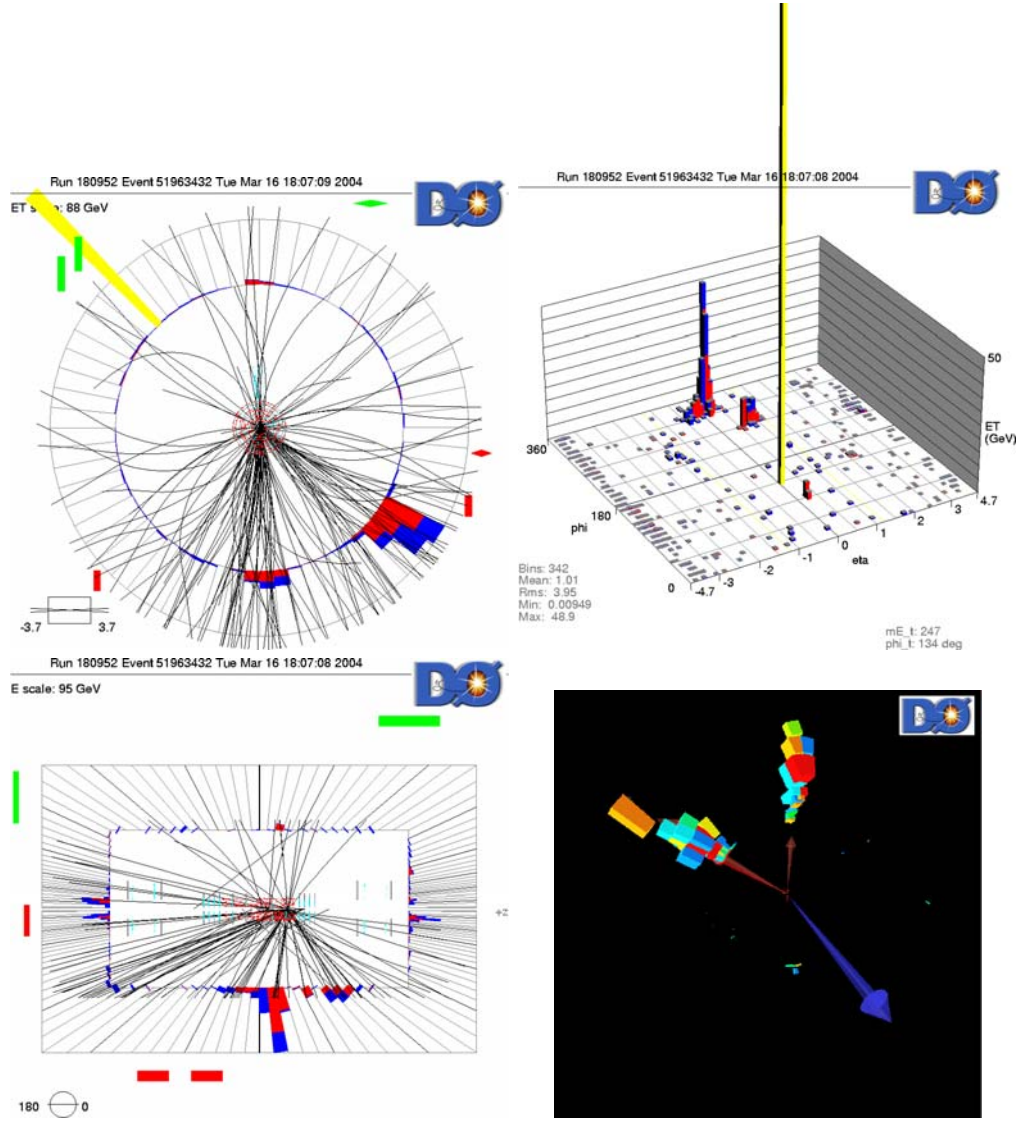


FIG. 6: Displays of the event with the largest missing E_T : xy view (top, left), lego plot (top, right), Rz view (bottom, left) and 3D-view (bottom, right).

- Missing Energy plus Multijets Signature*", Phys. Rev. Lett. **88** (2002) 041801.
- [3] H.P. Nilles, Phys. Rep. **110** (1984) 1.
 - [4] W. Beenakker, R. Hopker and M. Spira, "*PROSPINO: A program for the production of supersymmetric particles in next-to-leading order QCD*", [hep-ph/9611232]
 - [5] H. Baer, F.E. Paige, S.D. Protopopescu and X. Tata, "*ISAJET: A Monte Carlo Event Generator for pp , $\bar{p}p$, and e^+e^- Interactions*", hep-ph/0312045.
 - [6] The ALEPH, DELPHI, L3 and OPAL Collaborations and the LEP Working Group for Higgs boson searches, R. Barate *et al.*, "*Search for the Standard Model Higgs Boson at LEP*", Phys. Lett. **B565** (2003)61.